

# EVTAR: END-TO-END TRY ON WITH ADDITIONAL UNPAIRED VISUAL REFERENCE

A PREPRINT

Liuzhuozheng Li<sup>1,2\*</sup> Yue Gong<sup>2\*</sup> Shanyuan Liu<sup>2\*</sup> Bo Cheng<sup>2</sup> Yuhang Ma<sup>2</sup>  
 Liebucha Wu<sup>2</sup> Dengyang Jiang<sup>3</sup> Zanyi Wang<sup>4</sup> Dawei Leng<sup>2†</sup> Yuhui Yin<sup>2</sup>

<sup>1</sup>The University of Tokyo <sup>2</sup>360 AI Research

<sup>3</sup> Hong Kong University of Science and Technology <sup>4</sup>University of California San Diego.

Code is available at: <https://github.com/360CVGroup/EVTAR>

*End to end virtual tryon: Mapping target cloth onto the person without mask*



*End to end virtual tryon with additional visual references*



Figure 1: In-the-wild try-on results generated by our end-to-end EVTAR model, trained on person and garment images from our Virtual Fitting with Reference (VFR) dataset. The first row shows results obtained by directly transferring the garment to the target person, and the second row shows results generated with additional visual references.

## ABSTRACT

We propose **EVTAR**, an End-to-End Virtual Try-on model with Additional Reference, that directly fits the target garment onto the person image while incorporating reference images to enhance try-on accuracy. Most existing virtual try-on approaches rely on complex inputs such as agnostic person images, human pose, densepose, or body keypoints, making them labor-intensive and impractical for real-world applications. In contrast, EVTAR adopts a two-stage training strategy, enabling simple inference with only the source image and the target garment inputs. Our model generates try-on results without masks, densepose, or segmentation maps. Moreover, EVTAR leverages additional reference images of different individuals wearing the same clothes to preserve garment texture and fine-grained details better. This mechanism is analogous to how humans consider reference models when choosing outfits, thereby simulating a more realistic and high-quality dressing effect. To support these capabilities, we enrich the training data with supplementary references and unpaired person images. We evaluate EVTAR on two widely used benchmarks and diverse tasks, and the results consistently validate the effectiveness of our approach.

\*Equal Contribution

†Corresponding Author

## 1 Introduction

The virtual try-on(ViTTON) model aims to generate photo-realistic images of individuals wearing target clothing, with application scenarios including online retail, personalized fashion recommendation systems, and other fields. The ViTON methods can be broadly categorized into two types: Generative Adversarial Networks (GANs) [1] and diffusion models [2, 3]. Early studies typically relied on GANs [4–6]. They employed warping modules to deform clothing for alignment with the human body, followed by further fusion of the clothing and the human body to achieve visual harmony. However, such GAN-based methods generate unrealistic artifacts, especially when the clothing texture is complex or the human pose is challenging.

Recently, research based on latent diffusion models [7, 8] has gradually attracted attention in virtual try-on. Their powerful generation and editing capabilities have significantly improved clothing warping performance. Diffusion-based methods [9–12] significantly address issues related to structural arrangement and texture preservation during the denoising process, which the model requires. Nevertheless, current virtual try-on technologies based on diffusion models generally still rely on additional conditions, such as clothing regions masks, garment masks, human poses, key points, and inputs of other modalities such as text prompts [8, 13–16].

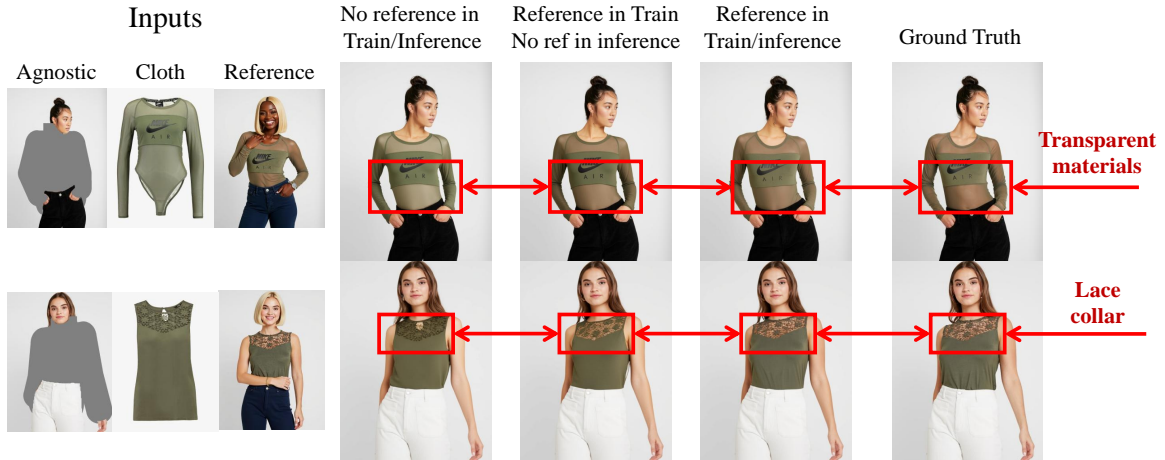


Figure 2: The effect of using reference images for the virtual try-on task. From left to right in the three middle subfigures are: (i) results generated without using reference images during either training or inference; (ii) results generated by a model trained with reference images but inferred without them; (iii) results generated by a model trained and inferred with reference images. Incorporating reference images consistently improves try-on detailed quality and authenticity in training and inference stages. Please zoom in for more details.

Despite the remarkable progress of prior virtual try-on approaches, they are still constrained by two critical limitations that hinder their authenticity of the try-on results and broader applicability: **First**, these approaches rely on multiple external models, such as pose estimators [17–21], human parse models [22, 23], segmentation models [24, 25], to process different conditions, which compromises the practicality. Moreover, in practical applications, the quality of conditional inputs—such as the cloth mask—has a substantial impact on the quality of the final try-on results; **Second**, many aspects of clothing, such as style, texture, and detailed design, cannot be fully perceived from the garment image alone; instead, it is more important to consider the overall appearance when the garment is worn by a model. Therefore, in real-world try-on scenarios, such as online shopping, users are typically more interested in model images rather than the garment itself. They tend to see how the target garment looks when worn on a real person, rather than relying solely on the isolated garment image as a reference. For example, as illustrated in Fig. 2, at the garment in first row, It is difficult to tell whether it is a green translucent fabric or a light green opaque one, whereas the reference image clearly reveals its green translucent material. We cannot accurately identify transparent materials or intricate designs, such as lace collars, solely from cloth images. In contrast, the reference images of human models wearing the garments reveal such details. However, existing virtual try-on methods do not support such references due to the lack of corresponding reference data in public datasets [26, 4, 27–31].

Based on the above observation, we propose **EVTAR**, an end-to-end virtual try-on framework that achieves strong performance *without relying on any external models or auxiliary components*, while being further enhanced by *additional reference images* that offer more accurate and context-aware guidance for the try-on model. First, EVTAR eliminates the need for auxiliary inputs such as segmentation masks, allowing for simple inference with only a source image and the target garment as inputs. Second, we introduce the use of images of a person clothed with the target

garment as the visual references, which better reflect users’ real-world behavior when choosing clothes and enable the preservation of fine garment details that existing methods cannot achieve. Furthermore, to achieve these objectives, we construct a new dataset with supplementary reference images and use end-to-end training to train our own model, which empowers EVTAR to achieve both simplified clothing replacement and higher-quality generation results.

In summary, the main contributions of this work are as follows:

- We propose **EVTAR**, a virtual try-on framework that transfers garments onto humans with or without auxiliary conditional information such as segmentation masks or dense pose. This design offers greater flexibility, significantly simplifies the model architecture, and enhances practicality for real-world applications.
- We introduce a novel method that incorporates reference model images for virtual try-on, which greatly enhances the authenticity and the quality of the try-on results. And we construct a high-quality dataset with supplementary reference images and unpaired person images to support our method.
- We provide a virtual try-on model that achieves state-of-the-art (SOTA) performance in both quantitative and qualitative evaluations, and also works well for in-the-wild person-cloth images, demonstrating the excellent capabilities of EVTAR.

## 2 Related Works

### 2.1 Generative Model via Flow Matching

Generative modeling has advanced rapidly, with diffusion models (DMs) [32], score-based generative models (SGMs) [33], and flow-based methods emerging as leading paradigms. Flow-based [34–36] methods have evolved to address inefficiencies in traditional continuous normalizing flows (CNFs)—which require expensive backpropagation through ODE solvers during training [37]—with a breakthrough being Flow Matching (FM) [38], which learns a time-dependent vector field to deterministically transport a simple prior distribution to the target data distribution, using a simulation-free training objective (unlike CNFs) that avoids numerical integration at training time to reduce computational overhead, and achieving comparable or superior sample quality to DMs with far fewer sampling steps (by directly parameterizing the probability flow instead of learning a stochastic reverse process [38]).

### 2.2 Diffusion-based Virtual Tryon

Diffusion models have advanced rapidly in recent years [2, 3], leading to a wide range of diffusion-based approaches in the virtual try-on domain [9, 10, 4]. Stable Diffusion [39, 9], with its flexible inpainting and text-guided capabilities, has become widely adopted for virtual try-on tasks. DiffusionCLIP [40] further incorporates CLIP loss to refine the generated images. DCI-VTON [41] follows a traditional two-stage pipeline, first warping clothing to align with the body and then fusing the warped garment with the person’s image. Subsequently, IDM-VTON [4] introduces a dedicated GarmentNet module that guides the garment structure and appearance, further improving visual realism. Despite these advances, diffusion-based virtual try-on methods still face notable limitations in practical application and technical completeness, leaving room for further research and optimization. In summary, existing diffusion-based virtual try-on methods either (1) rely on excessive auxiliary annotations or (2) lack support for reference images of clothed individuals. Our EVTAR model addresses these limitations by combining end-to-end diffusion training with reference-aided generation, while supporting mask-based inpaint or mask-free editing for virtual try-on.

## 3 Method

### 3.1 Preliminary

EVTAR is built upon DiT [42], a scalable Transformer architecture for diffusion-based generation. Images are encoded into a latent space via an autoencoder [43] and then patched into tokens [44]. The diffusion process [2] operates on these tokens, with the Transformer consuming noisy tokens and predicting their denoised results.

We consider the problem of generating images conditioned on an embedding  $\mathbf{y}$ , which may encode garment images, semantic maps, human pose, or other modality-specific control signals. Let  $\mathbf{x}$  denote the latent image representation obtained from a VAE encoder. The goal of **flux.1** [45, 46] is to approximate the conditional distribution  $p(\mathbf{x} | \mathbf{y})$  by learning a time-dependent velocity field  $\mathbf{v}(\mathbf{x}, \mathbf{y}, t)$  that transports a sample from a simple prior  $p_0(\mathbf{x}) = \mathcal{N}(\mathbf{0}, \mathbf{I})$  at  $t = 0$  to the data distribution  $p_{\text{data}}(\mathbf{x} | \mathbf{y})$  at  $t = 1$ . The dynamics of the conditional probability density  $p(\mathbf{x}, t | \mathbf{y})$  over

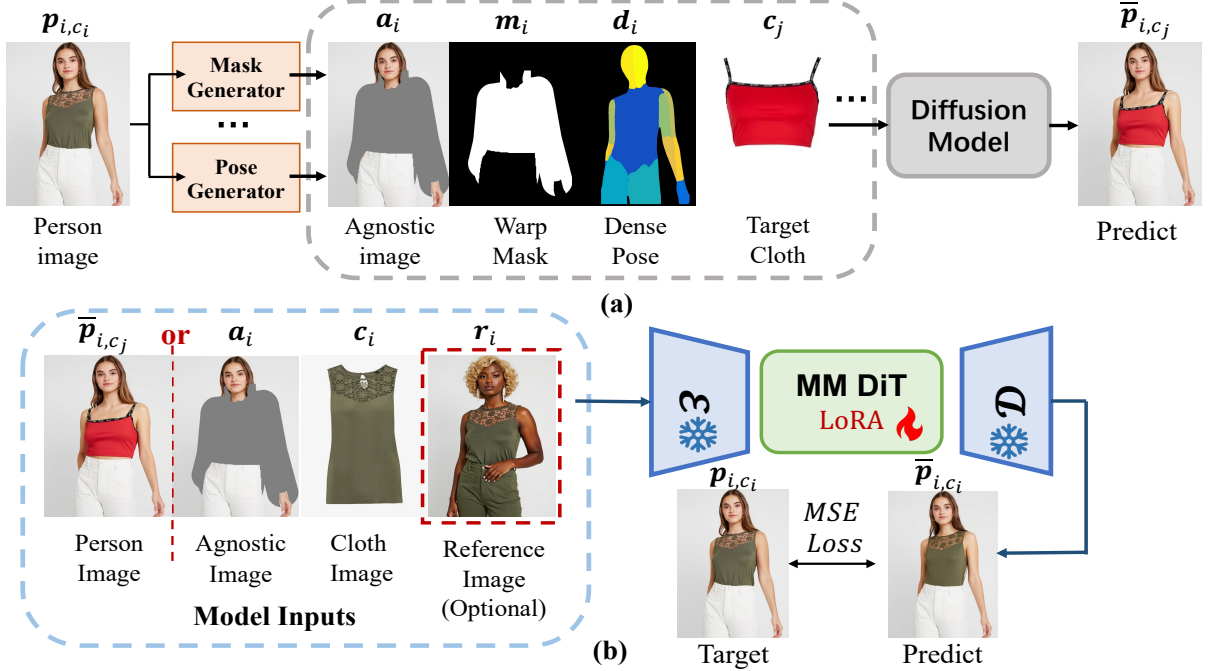


Figure 3: The pipeline of our two-stage training strategy: (a) In the first stage, which follows a similar paradigm to mask-based try-on approaches, the model is trained on masked person images to generate person images wearing random garments for the next stage training. (b) In the second stage, the synthesized person images produced from the first stage or agnostic image, the target garment, and the additional reference images(optional) are jointly used as inputs to train an end-to-end virtual try-on model that directly fits the target cloth onto the person’s body.

time  $t$  are governed by the continuity equation:

$$\frac{\partial}{\partial t} p(\mathbf{x}|\mathbf{y}, t) = -\nabla_{\mathbf{x}} \cdot (\mathbf{v}(\mathbf{x}, \mathbf{y}, t) \cdot p(\mathbf{x}|\mathbf{y}, t)), \quad \mathbf{x}_0 \sim p_0, \quad \mathbf{x}_1 \sim p_{\text{data}}. \quad (1)$$

To estimate  $\mathbf{v}(\mathbf{x}, \mathbf{y}, t)$ , we train a diffusion-transformer backbone to approximate the neural velocity field  $\mathbf{v}_{\theta}$  using the conditional flow matching objective [38, 47]:

$$\mathcal{L}_{\theta} = \mathbb{E}_{t, \mathbf{x}_i, \epsilon, \mathbf{y}_i} \left[ \|\mathbf{v}_{\theta}(\mathbf{x}, \mathbf{y}_i, t) - (\mathbf{x}_i - \epsilon)\|_2^2 \right], \quad \mathbf{x} = (1-t)\mathbf{x}_i + t\epsilon, \quad (2)$$

where  $t \sim \mathcal{U}(0, 1)$ ,  $\mathbf{x}_i \sim \mathcal{X}_{\text{train}}$ , and  $\epsilon \sim \mathcal{N}(\mathbf{0}, \mathbf{I})$ . This training objective encourages the model to learn a velocity field  $\mathbf{v}_{\theta}(\mathbf{x}, \mathbf{y}, t)$  that consistently guides the noisy samples toward the data distribution conditioned on  $\mathbf{y}$ , following the probability flow ODE starting from the Gaussian prior:

$$d\mathbf{x} = \mathbf{v}(\mathbf{x}, \mathbf{y}, t) dt, \quad (3)$$

enabling controllable image synthesis at inference time.

In the virtual try-on setting, let  $\mathbf{x}_i$  denote the image of a person wearing the target cloth, and let  $\mathbf{y}_i$  represent a collection of conditional inputs, including the cloth-agnostic image  $\mathbf{a}_i$ , the target cloth  $\mathbf{c}_i$ , the target person images  $\mathbf{p}_i$ , the visual references  $\mathbf{r}_i$ , and others. Formally, we write  $\mathbf{y}_i = [\mathbf{a}_i, \mathbf{c}_i, \mathbf{d}_i, \dots]$ . The objective is to progressively transform a Gaussian noise sample  $\epsilon$  into the target image  $\mathbf{x}_i$  guided by conditions  $\mathbf{y}_i$ .

### 3.2 End To End Virtual Try-on Model with Two Stage Training

Unlike previous methods that first mask the target cloth region to generate an agnostic image, our objective is to design a model that can directly fit the target cloth onto the target person, without introducing additional conditions such as densepose [17] or segmentation masks. To this end, we train a diffusion model on pairs of cloth images  $\mathbf{c}_i$  and person images wearing different clothes  $\mathbf{p}_i$ , as illustrated in Fig. 3 (b).

To train a model capable of directly taking a person’s image as input rather than relying on a segmentation mask and masked agnostic images, it is necessary to construct a training set containing unpaired person images of the form

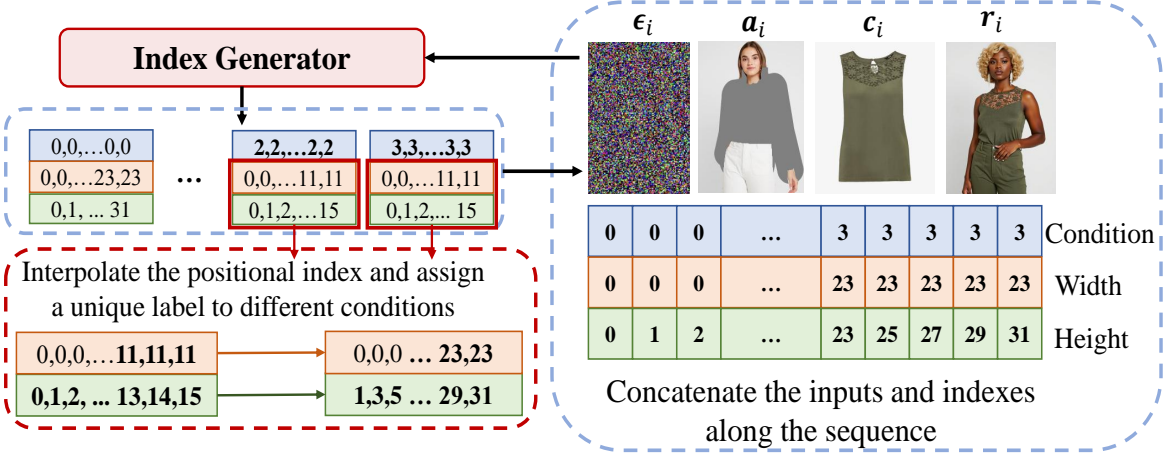


Figure 4: Generating the tryon result with additional visual reference. We train a tryon model conditioned on cloth  $c_i$ , reference image  $r_i$ , and takes agnostic  $a_i$  or reference image  $r_i$  as input to fit the cloth image onto the target person.

“the same person wearing different clothes,” denoted as  $[\bar{p}_{i,c_j}, c_i, p_{i,c_i}]$ , where the subscript  $c_j$  of  $\bar{p}_{i,c_j}$  indicates the garment other than  $c_i$  being worn. Unfortunately, collecting such unpaired cloth–person data pairs  $[\bar{p}_{i,c_j}, c_i, p_{i,c_i}]$  from the real world is challenging, and these unpaired examples are not available in current open-source benchmarks sense most of them only contain data pair  $[c_i, p_{i,c_i}]$ . Therefore, we first synthesize unpaired person images  $\bar{p}_{i,c_j}$  using a mask-based try-on model, which serves as the first stage of our EVTAR training strategy. As illustrated in Fig. 3(a), we train a virtual try-on model using agnostic person images  $a_i$ , clothing images  $c_i$ , densepose maps  $d_i$ , warp masks  $mi$ , and other auxiliary conditions as inputs. During inference, a random unpaired garment  $c_j$  is selected to generate the corresponding synthesized person image  $\bar{p}_{i,c_j}$ . To ensure the quality of the synthesized person image  $\bar{p}_{i,c_j}$ , the agnostic–cloth pairs  $[a_i, c_i]$  used for training must belong to the same garment category (e.g., if  $a_i$  is from the “dresses” subset, the selected garment  $c_j$  should also come from “dresses” rather than “upper body” or “lower body”). Otherwise, the generated person image may appear unrealistic due to mismatches between the clothing mask region and the target garment (e.g., fitting a skirt onto the upper body or a shirt onto the lower body).

### 3.3 Muti-input Adaptation of EVTAR

After obtaining the unpaired person images, we train our end-to-end model by replacing the agnostic images  $a_i$  with the corresponding person images  $p_i$ , which are generated by the first stage model. To enable the model to handle both masked and unmasked inputs flexibly, we randomly feed agnostic and person images with equal probability (50%) during training. Instead of training a try-on model from scratch, we adopt *Flux-Kontext* [46] as the foundation model, freeze the parameters of its encoder and decoder, and apply Low-Rank Adaptation (LoRA) [48] to the MM-DiT blocks for parameter-efficient fine-tuning. The training objective follows the same flow-matching loss as defined in Equation 2, where  $a_i$  and  $p_i$  are alternately used to ensure compatibility with both input types. To enable the model to extract visual information from the target garment worn by another person, an additional reference image  $r_i$  is provided as input with a certain probability (25%). Its latent embeddings are appended to the latent feature sequence  $[\epsilon_i, a_i, c_i]$  after the image encoder, as illustrated in Fig. 3(b).

The *Flux-Kontext* architecture provides a flexible framework for image editing. The input image is first converted into latent embeddings by the image encoder and then flattened into a sequence of shape  $[L, D]$ , where  $L$  denotes the sequence length per image and  $D$  is the embedding dimension. This sequence is concatenated with the Gaussian noise  $\epsilon$  along the sequence dimension. Similar to a Vision Transformer that employs positional embeddings to encode spatial information, *Flux-Kontext* uses an index generator to produce a positional index of shape  $[L, 3]$  for the image embedding sequence. These indices are subsequently transformed into Rotary Positional Embeddings (RoPE), providing additional spatial cues to the model. The first channel of the positional index indicates whether the embedding corresponds to Gaussian noise  $\epsilon_i$  or conditional inputs, while the second and third channels represent the horizontal and vertical positional indices, respectively, as illustrated in Fig. 4.

Based on this design, we first convert the conditional inputs into latent embeddings with a shape of  $[L, D]$ , denoted as  $[a_i, c_i, r_i]$ , and concatenate them with the Gaussian noise embeddings  $\epsilon_i$  along the sequence dimension. However, the vanilla *Flux-Kontext* [46] supports only a single conditional image input, which is insufficient for virtual try-on tasks that require at least the target person  $p_i$  and the garment  $c_i$ . To overcome this limitation, we extend the positional index

for RoPE used by the DiT blocks. Each embedding is assigned a three-channel index: the first channel, originally binary (0 for noise and 1 for condition), is expanded to values from 0 to 3 to distinguish multiple conditional inputs; the second and third channels encode horizontal and vertical positions as integers. To support multi-resolution conditions, we further scale the positional indices in the second and third channels according to the resolution ratio between the target and conditional images, ensuring that all indices remain within a consistent numerical range. The modified positional index design of the DiT blocks and the overall architecture of our EVTAR are illustrated in Fig. 4.

### 3.4 Virtual-Tryon Generation with Extra Visual Reference

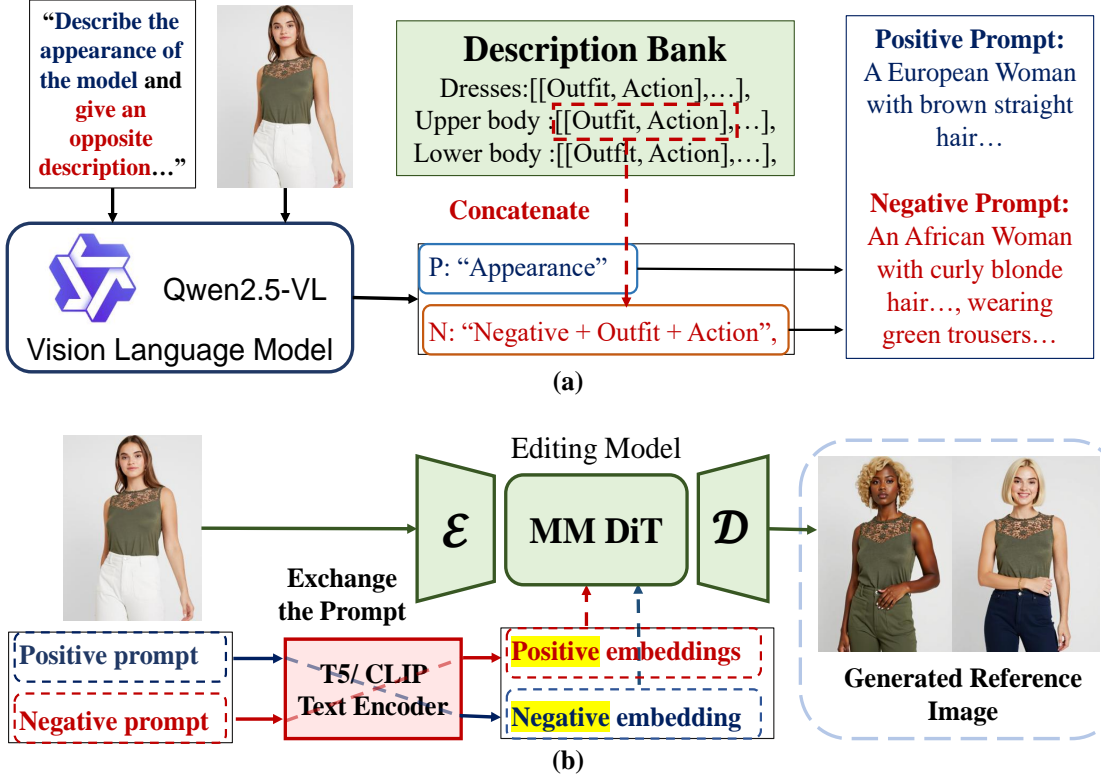


Figure 5: The overall pipeline of generating the reference images. We first generate the appearance descriptions using *Qwen2.5-VL* [49], and then concatenate the appearance with the corresponding actions and outfits to construct the positive and negative prompts, as shown in (a). Subsequently, the images and the textual prompts are fed into the Editing Model, which generates photos of individuals wearing the same clothes. These results are reference images for each image-cloth pair, as shown in (b).

For humans, particularly in e-commerce shopping, we believe that relying solely on garment images and conditions extracted by external models, as done in previous methods, is insufficient to imagine the realistic visual effects of fitting a target garment onto one’s body. A garment’s style, texture, and fine design elements are more faithfully represented when worn by another person, whereas viewing the garment in isolation fails to convey these nuances. The same applies to generative virtual try-on models, as illustrated in Fig. 2. Therefore, we argue that relying on cloth images and conditions extracted by external models, as in previous methods, is insufficient to capture the realistic visual effect of fitting a target garment onto a person. By incorporating reference person images, **that the target clothes worn by another person  $r_i$** , into the virtual try-on generation process, the model can similarly get more intuitive visual guidance.

To provide the model with reference person images  $r_i$ , we construct pairs in the form of “different persons wearing the target garment,” denoted as  $[c_i, r_i]$ . Such reference images  $r_i$  are not available in existing open-source virtual try-on datasets, similar to the person images  $p_i$ . In this subsection, we introduce our data engine, which synthesizes the required reference images, enriching current virtual try-on datasets with supplementary references and enabling our model to be trained with additional visual guidance.

Existing open-source datasets, including **VITON-HD** [4], **DressCode** [26], and **IGPairs** [29], lack unpaired reference images  $r_i$  showing *the different persons wearing the target garment*, thereby constraining the model’s training. We

employ generative models to synthesize such reference images to overcome this limitation. For the generated reference data  $r_i$  to provide accurate and intuitive visual guidance, we argue that they should meet the following requirements:

1. **Preserve the target garment faithfully.** The target clothing’s color, texture, and design must remain unchanged to ensure accurate reference.
2. **Introduce diversity in person identity.** The person wearing the target garment in the reference image should not be identical to the target person wearing the same garment. Otherwise, the model may overfit to the target image. This diversity can be achieved by altering hairstyle, hair/skin color, body pose, or facial expressions.
3. **Vary the non-target garments.** While the target garment remains unchanged, other garments should be modified. For example, if the target garment is an upper-body item, the reference image should retain the same upper-body garment but alter the lower-body clothing, shoes, or accessories.

The overall generation pipeline for reference data is illustrated in Figure 5.

As shown in the pipeline, we employ **Flux-Kontext** [46] to generate reference images from the target descriptions, leveraging its strong capability to maintain consistency with the input image (1). To address requirement (2), we describe the target image and then intentionally provide an alternative description that ensures the reference image differs from the target input. For this purpose, we use **Qwen2.5-VL** [49] to generate detailed descriptions of the model’s appearance, and instruct it to produce variants that do not resemble the original model. Finally, to fulfill requirement (3), we curate a list of garment descriptions representing diverse non-target clothing items. The outlook, action, and outfit descriptions are concatenated as the *positive prompt*. In contrast, the original image description is used as the *negative prompt*, and both are fed into the generative model to synthesize reference images.

We supplement existing virtual try-on benchmarks including **VITON-HD** [5], **DressCode** [26], **ViViD** [27], **FashionTryOn** [28] and **IGPairs** [29] by generating corresponding reference pairs for each target garment image  $c_i$ , forming data pairs  $[c_i, r_i]$  that are used for both model training and evaluation. Some open-source datasets, such as **FashionTryOn** [28] and **IGPairs** [29], contain numerous duplicated or low-quality samples. We filter out redundant or poor-quality images to ensure overall data quality before generating the final reference data using our data engine. Finally, we enrich open-source virtual try-on datasets with additional visual references  $r_i$  and person images  $p_i$ , and combine them to form our own dataset, named **Virtual Fitting with Reference (VFR)**, for training our EVTAR model.

## 4 Experiments

We evaluate the effectiveness of our proposed method on two public benchmarks, **DressCode** [26] and **VITON-HD** [4], both containing images with a resolution of  $1024 \times 768$ . The VITON-HD dataset comprises 13,670 upper-body image pairs of women, split into 11,647 pairs for training and 2,032 pairs for testing. The DressCode dataset includes three subsets—upper body, lower body, and dresses—with 48,392 training and 5,400 testing pairs. Since DressCode does not provide wrapped cloth masks or agnostic images  $a_i$ , we generate them using the mask generation tool from CatVTN [14]. During training, we fine-tune our model on the *flux-kontext* backbone using the Low-Rank Adaptation (LoRA) technique, with a rank of 64 and  $\alpha = 128$ , optimized by *AdamW*. For quantitative evaluation, all generated images are resized to  $512 \times 384$  to ensure a fair comparison with previous methods. In a single-dataset experiment, the model is trained independently for 20,000 steps on VITON-HD and 48,000 on DressCode with a batch size of 128, using 8 NVIDIA H100 GPUs. To further enhance generalization and robustness to in-the-wild inputs, we train an additional model on the mixed VFR dataset introduced in Sec. 3.4. We report cross-dataset evaluation results of our EVTAR model at a resolution of  $1024 \times 768$  on both VITON-HD and DressCode, and demonstrate its in-the-wild performance using images captured by ourselves and collected from the internet.

### 4.1 Quantitative result

We evaluate the numerical results of our virtual try-on model on the VITON and DressCode datasets, distinguishing between paired and unpaired try-on settings. For paired try-on settings with ground truth in test datasets, we utilize four widely used metrics to assess the similarity between the synthesized images and their corresponding authentic images: the Structural Similarity Index (**SSIM**) [50], Learned Perceptual Image Patch Similarity (**LPIPS**) [51], Fréchet Inception Distance (**FID**) [52], and Kernel Inception Distance (**KID**) [53]. For unpaired settings, where we measure the distributional similarity between the synthesized and real samples, we specifically rely on the **Fréchet Inception Distance (FID)** and **Kernel Inception Distance (KID)**. As shown in Table 1.

Our method (**EVTAR**) consistently performs better than prior baselines, demonstrating higher try-on fidelity and strong alignment with the target person’s pose. With the addition of reference images (“+R”), the quality and detail

Table 1: Quantitative results on the VITON-HD dataset [4]. The best and second best results are reported in **bold** and underline, respectively. The \* marker refers to the results reported in previous work. The symbol “+R” denotes results with reference image input, and “MF” indicates *mask-free* input images. Subscripts  $p$  and  $u$  represent the *paired* and *unpaired* test settings, respectively. In the *Input* columns, a “ $\checkmark$ ” symbol indicates that the model requires the corresponding input, while “–” means it does not.

Method	Input			LPIPS $_{p\downarrow}$	SSIM $_{p\uparrow}$	FID $_{p\downarrow}$	KID $_{p\downarrow}$	FID $_{u\downarrow}$	KID $_{u\downarrow}$
	Mask	Pose	Prompt						
CAT-DM* [54]	✓	✓	–	0.080	0.877	5.60	0.83	8.93	1.37
IDM-VTON* [12]	✓	✓	✓	0.102	0.870	6.29	–	–	–
OOTDiffusion* [8]	✓	–	–	0.071	0.878	8.81	<u>0.82</u>	–	–
CatVTON* [14]	✓	–	–	0.057	0.870	5.43	0.41	9.02	1.09
CatVT2ON* [15]	✓	✓	–	0.057	0.890	8.10	2.25	11.22	2.99
OmniVTON* [16]	✓	✓	✓	0.145	0.832	7.76	–	9.62	–
PromptDresser <sub>pose</sub> * [13]	✓	✓	✓	0.097	<u>0.878</u>	9.07	1.16	–	–
PromptDresser* [13]	✓	–	✓	0.112	0.869	8.54	<b>0.67</b>	–	–
EVTAR(Ours)	✓	–	–	0.057	0.873	<u>5.45</u>	<u>0.82</u>	8.58	1.06
EVTAR+R(Ours)	✓	–	–	<b>0.049</b>	<b>0.879</b>	<b>4.69</b>	0.68	8.43	0.91
EVTAR/MF (Ours)	–	–	–	0.061	0.866	5.98	1.04	<u>8.40</u>	<u>0.81</u>
EVTAR+R/MF(Ours)	–	–	–	<u>0.053</u>	0.872	5.11	<u>0.82</u>	<b>8.32</b>	<b>0.78</b>

consistency of the try-on results is further improved compared with the results without reference images, establishing new state-of-the-art results across multiple metrics. Notably, even in the mask-free setting—without agnostic masks or auxiliary inputs—our method maintains garment style correctness and pose consistency, while reaching accuracy on par with or superior to baseline methods, highlighting its robustness and practicality.

Table 2: Quantitative results on the DressCode dataset [26]. The best and second best results are reported in **bold** and underline, respectively. The \* marker refers to the results reported in previous work. The symbol “+R” denotes results with reference image input, and “MF” indicates *mask-free* input images. Subscripts  $p$  and  $u$  represent the *paired* and *unpaired* test settings, respectively.

Method	All					
	LPIPS $_{p\downarrow}$	SSIM $_{p\uparrow}$	FID $_{p\downarrow}$	KID $_{p\downarrow}$	FID $_{u\downarrow}$	KID $_{u\downarrow}$
IDM-VTON* [4]	0.062	0.920	8.64	0.90	–	–
OOTDiffusion* [8]	0.045	<b>0.927</b>	4.20	<b>0.37</b>	–	–
CatVTON* [14]	0.046	0.892	3.99	<u>0.82</u>	6.14	1.40
CatVT2ON* [15]	0.037	<u>0.922</u>	5.72	2.34	8.63	3.84
OmniVTON* [16]	0.119	0.865	5.34	–	6.45	–
EVTAR(Ours)	0.037	0.912	<u>3.48</u>	1.20	5.31	1.36
EVTAR+R(Ours)	<b>0.031</b>	0.918	<b>2.94</b>	0.95	5.07	<b>1.15</b>
EVTAR/MF (Ours)	0.041	0.901	3.84	1.33	<b>5.00</b>	<u>1.17</u>
EVTAR+R/MF(Ours)	<u>0.035</u>	0.906	3.34	1.15	<u>5.02</u>	1.28

Table 2 and Table 3 summarizes the quantitative evaluation on the DressCode dataset. Our method (EVTAR) outperforms all baselines, delivering higher try-on quality and achieving strong consistency with the target person’s pose and body structure. Integrating reference images (“+R”) further enhances the results, establishing a new state-of-the-art. Importantly, even in the mask-free setting—without agnostic masks or additional inputs—our method correctly preserves garment styles (e.g., clothing length and design) and maintains high pose alignment, while achieving accuracy comparable to or surpassing prior baselines, demonstrating robustness and practicality.

## 4.2 QUALITATIVE COMPARISON

Although the previous method can fit the garment onto a human body, the generated results often fail to accurately capture the garment’s cut, style, details, and other characteristics that determine how it should be worn. In contrast, our method achieves superior visual fidelity compared to baselines. As shown in Fig. 6, on the VITON dataset, our

Table 3: Quantitative results on different subsets of the Dress Code dataset [26]. The best and second best results are reported in **bold** and underline, respectively. The \* marker refers to the results reported in previous work. The symbol “+R” denotes results with reference image input, and “MF” indicates *mask-free* input images. Subscripts  $p$  and  $u$  represent the *paired* and *unpaired* test settings, respectively.

Method	Upper-body				Lower-body				Dresses			
	$\text{FID}_{p\downarrow}$	$\text{KID}_{p\downarrow}$	$\text{FID}_{u\downarrow}$	$\text{KID}_{u\downarrow}$	$\text{FID}_{p\downarrow}$	$\text{KID}_{p\downarrow}$	$\text{FID}_{u\downarrow}$	$\text{KID}_{u\downarrow}$	$\text{FID}_{p\downarrow}$	$\text{KID}_{p\downarrow}$	$\text{FID}_{u\downarrow}$	$\text{KID}_{u\downarrow}$
CAT-DM* [54]	9.85	2.38	12.62	1.89	10.25	1.81	14.83	2.82	10.71	2.02	14.30	3.36
OOTDiffusion* [8]	11.03	0.29	—	—	9.72	0.64	—	—	10.65	0.54	—	—
PromptDresser* [13]	11.00	0.74	—	—	12.55	1.46	—	—	11.09	1.10	—	—
EVTAR(Ours)	<u>7.62</u>	<u>1.10</u>	<u>11.13</u>	<u>0.98</u>	<u>7.60</u>	1.38	13.07	2.11	7.32	1.30	11.56	1.98
EVTAR+R(Ours)	<b>6.39</b>	<b>0.85</b>	<b>11.08</b>	<b>0.87</b>	<b>6.61</b>	<b>1.05</b>	<u>12.56</u>	<b>1.67</b>	<b>6.09</b>	<b>1.16</b>	11.16	1.72
EVTAR/MF(Ours)	8.37	1.43	11.20	1.11	8.79	1.51	<b>12.50</b>	<u>1.83</u>	7.36	1.33	<u>10.73</u>	<u>1.41</u>
EVTAR+R/MF(Ours)	<u>7.20</u>	1.18	11.53	1.12	7.85	<u>1.21</u>	12.74	2.05	<u>6.24</u>	<u>1.20</u>	<b>10.05</b>	<b>1.30</b>

EVTAR produces a highly realistic rendering of challenging garment materials such as hollow or semi-transparent fabrics without relying on reference images. For example, in the case of garments with hollow lace structures, our model accurately preserves the delicate perforated patterns and material transparency. In contrast, the baselines fail to reconstruct these details, often generating incorrect solid textures or spurious dotted patterns. Moreover, our approach demonstrates the best preservation of garment patterns: the printed letters and logos on clothes remain clear and consistent with the input, highlighting its advantage in maintaining fine-grained appearance details. The generation quality is further enhanced with the addition of reference images, which intuitively verify the effectiveness of the proposed tryon method. Even without using agnostic masks and by directly transferring the clothing  $c_i$  onto person images  $\bar{p}_{i,c_j}$ , our method still outperforms most baseline approaches.

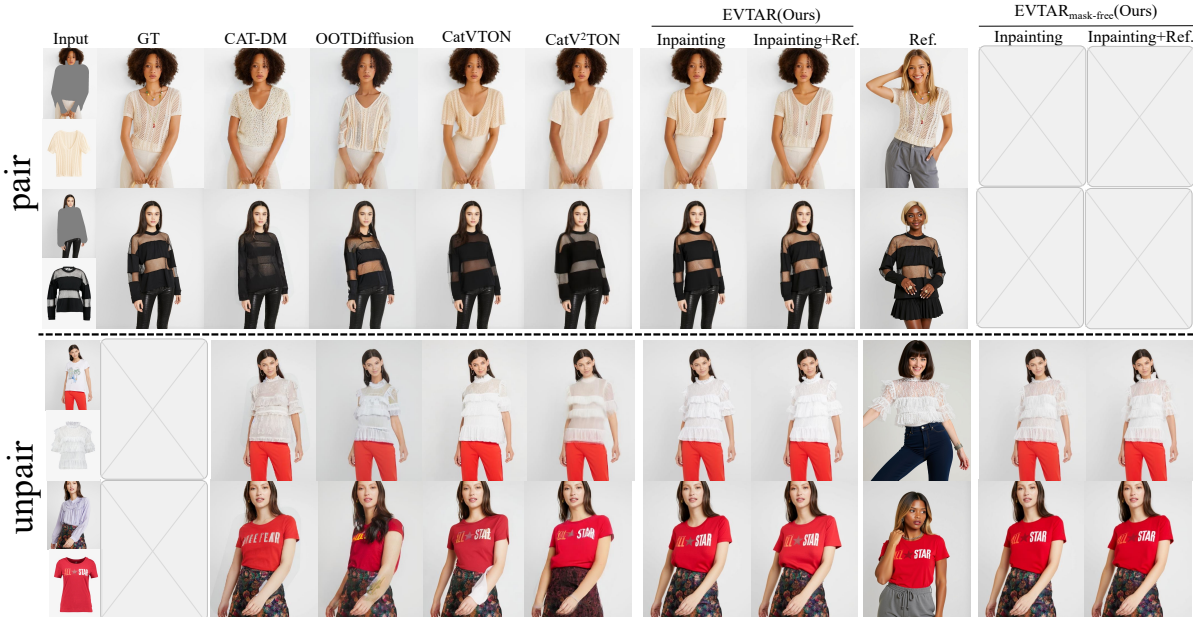


Figure 6: Qualitative comparison on the VITON dataset. and the model is trained following the pipeline in Fig. 3 (b). “Ref” denotes the additional reference  $r_i$  image is used during the inference, while “mask-free” indicates that the image is generated using an unmasked person  $p_i$  image instead of a masked agnostic image  $a_i$ .

Our model also performs well on a benchmark comprising a wider variety of clothing types. As shown in Fig. 7, we evaluate our method on the DressCode dataset, where garments are categorized into three types: *upper body*, *lower body*, and *dresses*. Our approach produces more faithful and natural try-on results compared to previous methods. In particular, it renders reflective materials such as leather and metallic fabrics with superior realism, avoiding the over-smoothing or distortion artifacts commonly observed in other methods. Moreover, even without agnostic masks, our model can still perform consistent try-on guided by garment style, accurately preserving the length, structure, and overall design without introducing mismatched or inconsistent clothing shapes.



Figure 7: **Qualitative comparison on the DressCode dataset.**, and the model is trained following the pipeline in Fig. 3 (b). “Ref.” denotes the additional reference  $r_i$  image is used during the inference, while “mask-free” indicates that the image is generated using an unmasked person  $p_i$  image instead of a masked agnostic image  $a_i$ .

### 4.3 Training on VRF Dataset and Evaluation

Table 4: We compare our approach with [8] under cross-dataset evaluation, reporting results on both paired and unpaired settings for the VITON-HD and DressCode datasets. The best results are highlighted in **bold**. The \* marker refers to the results reported in previous work. The symbol “+R” denotes results with reference image input, and “MF” indicates *mask-free* input images. Subscripts  $p$  and  $u$  represent the *paired* and *unpaired* test settings, respectively.

Methods	VITON-HD						DressCode					
	SSIM $\uparrow$	FID $_{p\downarrow}$	KID $_{p\downarrow}$	LPIPS $\downarrow$	FID $_{u\downarrow}$	KID $_{u\downarrow}$	SSIM $\uparrow$	FID $_{p\downarrow}$	KID $_{p\downarrow}$	LPIPS $\downarrow$	FID $_{u\downarrow}$	KID $_{u\downarrow}$
OOTDiffusion* [8]	0.839	11.22	2.72	0.123	—	—	0.915	11.96	1.21	0.061	—	—
EVTAR(Ours)	0.851	6.23	0.80	0.072	9.11	1.08	0.896	3.70	1.13	0.045	5.22	1.20
EVTAR+R(Ours)	<b>0.859</b>	<b>5.13</b>	<b>0.62</b>	<b>0.060</b>	8.59	0.87	<b>0.903</b>	<b>3.14</b>	<b>0.97</b>	<b>0.038</b>	5.03	1.11
EVTAR/MF(Ours)	—	—	—	—	8.88	0.82	—	—	—	—	5.03	1.23
EVTAR+R/MF(Ours)	—	—	—	—	<b>8.39</b>	<b>0.65</b>	—	—	—	—	<b>4.87</b>	<b>1.10</b>

To better evaluate the effectiveness of our proposed end-to-end virtual try-on framework and data construction method, we construct a mixed dataset, *Mixed-Virtual-Ref*, by combining data from DressCode, VITON-HD, FashionTryOn [55], ViViD [27], and IGPairs [12]. We carefully select high-quality samples using *Qwen2.5-VL* to filter out low-quality target images, generate cloth-agnostic images with the mask generator from [14], and produce reference and unpaired person images using our data engine. We collect 103,936 image pairs to train our end-to-end virtual try-on model. The training hyperparameters are consistent with those used in the DressCode and VITON-HD experiments. We also

evaluate the model on the DressCode and VITON-HD test sets, with quantitative results reported in Table 4. Our method (EVTAR) consistently achieves superior or comparable performance to OOTDiffusion [8] across both VITON-HD and DressCode benchmarks under paired and unpaired settings. Although EVTAR is not explicitly trained on DressCode or VITON-HD, the model trained on the mixed VRF dataset outperforms dataset-specific baselines across most metrics (e.g., FID and LPIPS), demonstrating a strong generalization capability. These results highlight the effectiveness of our approach in learning transferable representations that maintain robustness across diverse datasets.

## 5 Conclusion

In this work, inspired by the human painting process, we design a diffusion model that generates high-quality, class-conditional samples without relying on time or class embeddings by mitigating manifold overlap through geometric decoupling of timesteps. The proposed approach simplifies diffusion models and effectively overcomes the challenges introduced by removing time conditioning, while preserving generation performance. More broadly, we offer a novel geometric perspective to understand the dynamics of diffusion processes in high-dimensional data spaces, inspired by the inherent sparsity of data distributions in high-dimensional statistics. We anticipate that our theoretical insights will inspire future research to simplify diffusion-based models by eliminating time and class embeddings and reducing their training and parametric complexity.

## References

- [1] Ian Goodfellow, Jean Pouget-Abadie, Mehdi Mirza, Bing Xu, David Warde-Farley, Sherjil Ozair, Aaron Courville, and Yoshua Bengio. Generative adversarial networks. *Communications of the ACM*, 63(11):139–144, 2020.
- [2] Jonathan Ho, Ajay Jain, and P. Abbeel. Denoising diffusion probabilistic models. *ArXiv*, abs/2006.11239, 2020. URL <https://api.semanticscholar.org/CorpusID:219955663>.
- [3] Robin Rombach, A. Blattmann, Dominik Lorenz, Patrick Esser, and Björn Ommer. High-resolution image synthesis with latent diffusion models. *2022 IEEE/CVF Conference on Computer Vision and Pattern Recognition (CVPR)*, pages 10674–10685, 2021. URL <https://api.semanticscholar.org/CorpusID:245335280>.
- [4] Seunghwan Choi, Sunghyun Park, Minsoo Lee, and Jaegul Choo. Viton-hd: High-resolution virtual try-on via misalignment-aware normalization. In *Proceedings of the IEEE/CVF conference on computer vision and pattern recognition*, pages 14131–14140, 2021.
- [5] Xintong Han, Zuxuan Wu, Zhe Wu, Ruichi Yu, and Larry S Davis. Viton: An image-based virtual try-on network. In *Proceedings of the IEEE conference on computer vision and pattern recognition*, pages 7543–7552, 2018.
- [6] Bochao Wang, Huabin Zheng, Xiaodan Liang, Yimin Chen, Liang Lin, and Meng Yang. Toward characteristic-preserving image-based virtual try-on network. In *Proceedings of the European conference on computer vision (ECCV)*, pages 589–604, 2018.
- [7] Mengting Chen, Xi Chen, Zhonghua Zhai, Chen Ju, Xuewen Hong, Jinsong Lan, and Shuai Xiao. Wear-any-way: Manipulable virtual try-on via sparse correspondence alignment. In *European Conference on Computer Vision*, pages 124–142. Springer, 2024.
- [8] Yuhao Xu, Tao Gu, Weifeng Chen, and Chengcai Chen. Ootdiffusion: Outfitting fusion based latent diffusion for controllable virtual try-on. In *AAAI Conference on Artificial Intelligence*, 2024. URL <https://api.semanticscholar.org/CorpusID:268247604>.
- [9] Jeongho Kim, Guojung Gu, Minho Park, Sunghyun Park, and Jaegul Choo. Stableviton: Learning semantic correspondence with latent diffusion model for virtual try-on. In *Proceedings of the IEEE/CVF conference on computer vision and pattern recognition*, pages 8176–8185, 2024.
- [10] Luyang Zhu, Dawei Yang, Tyler Zhu, Fitsum Reda, William Chan, Chitwan Saharia, Mohammad Norouzi, and Ira Kemelmacher-Shlizerman. Tryondiffusion: A tale of two unets. In *Proceedings of the IEEE/CVF conference on computer vision and pattern recognition*, pages 4606–4615, 2023.
- [11] Zhongcong Xu, Jianfeng Zhang, Jun Hao Liew, Hanshu Yan, Jia-Wei Liu, Chenxu Zhang, Jiashi Feng, and Mike Zheng Shou. Magicanimate: Temporally consistent human image animation using diffusion model. In *Proceedings of the IEEE/CVF Conference on Computer Vision and Pattern Recognition*, pages 1481–1490, 2024.
- [12] Yisol Choi, Sangkyung Kwak, Kyungmin Lee, Hyungwon Choi, and Jinwoo Shin. Improving diffusion models for authentic virtual try-on in the wild. In *European Conference on Computer Vision*, pages 206–235. Springer, 2024.
- [13] Jeongho Kim, Hoeyeong Jin, Sunghyun Park, and Jaegul Choo. Promptdresser: Improving the quality and controllability of virtual try-on via generative textual prompt and prompt-aware mask. *arXiv preprint arXiv:2412.16978*, 2024.

[14] Zheng Chong, Xiao Dong, Haoxiang Li, Shiyue Zhang, Wenqing Zhang, Xujie Zhang, Hanqing Zhao, Dongmei Jiang, and Xiaodan Liang. Catvton: Concatenation is all you need for virtual try-on with diffusion models. *arXiv preprint arXiv:2407.15886*, 2024.

[15] Zheng Chong, Wenqing Zhang, Shiyue Zhang, Jun Zheng, Xiao Dong, Haoxiang Li, Yiling Wu, Dongmei Jiang, and Xiaodan Liang. Catv2ton: Taming diffusion transformers for vision-based virtual try-on with temporal concatenation. *arXiv preprint arXiv:2501.11325*, 2025.

[16] Zhaotong Yang, Yuhui Li, Shengfeng He, Xinzhe Li, Yangyang Xu, Junyu Dong, and Yong Du. Omnitvton: Training-free universal virtual try-on. *arXiv preprint arXiv:2507.15037*, 2025.

[17] Rıza Alp Güler, Natalia Neverova, and Iasonas Kokkinos. Densepose: Dense human pose estimation in the wild. In *Proceedings of the IEEE conference on computer vision and pattern recognition*, pages 7297–7306, 2018.

[18] Alexander Toshev and Christian Szegedy. Deeppose: Human pose estimation via deep neural networks. In *Proceedings of the IEEE conference on computer vision and pattern recognition*, pages 1653–1660, 2014.

[19] Z. Cao, G. Hidalgo Martinez, T. Simon, S. Wei, and Y. A. Sheikh. Openpose: Realtime multi-person 2d pose estimation using part affinity fields. *IEEE Transactions on Pattern Analysis and Machine Intelligence*, 2019.

[20] Zhe Cao, Tomas Simon, Shih-En Wei, and Yaser Sheikh. Realtime multi-person 2d pose estimation using part affinity fields. In *CVPR*, 2017.

[21] Shih-En Wei, Varun Ramakrishna, Takeo Kanade, and Yaser Sheikh. Convolutional pose machines. In *CVPR*, 2016.

[22] Peike Li, Yunqiu Xu, Yunchao Wei, and Yi Yang. Self-correction for human parsing. *IEEE Transactions on Pattern Analysis and Machine Intelligence*, 2020. doi:[10.1109/TPAMI.2020.3048039](https://doi.org/10.1109/TPAMI.2020.3048039).

[23] Jian Dong, Qiang Chen, Xiaohui Shen, Jianchao Yang, and Shuicheng Yan. Towards unified human parsing and pose estimation. In *Proceedings of the IEEE Conference on Computer Vision and Pattern Recognition*, pages 843–850, 2014.

[24] Alexander Kirillov, Eric Mintun, Nikhila Ravi, Hanzi Mao, Chloe Rolland, Laura Gustafson, Tete Xiao, Spencer Whitehead, Alexander C Berg, Wan-Yen Lo, et al. Segment anything. In *Proceedings of the IEEE/CVF international conference on computer vision*, pages 4015–4026, 2023.

[25] Nikhila Ravi, Valentin Gabeur, Yuan-Ting Hu, Ronghang Hu, Chaitanya Ryali, Tengyu Ma, Haitham Khedr, Roman Rädle, Chloe Rolland, Laura Gustafson, Eric Mintun, Junting Pan, Kalyan Vasudev Alwala, Nicolas Carion, Chao-Yuan Wu, Ross Girshick, Piotr Dollár, and Christoph Feichtenhofer. Sam 2: Segment anything in images and videos. *arXiv preprint arXiv:2408.00714*, 2024. URL <https://arxiv.org/abs/2408.00714>.

[26] Davide Morelli, Matteo Fincato, Marcella Cornia, Federico Landi, Fabio Cesari, and Rita Cucchiara. Dress code: High-resolution multi-category virtual try-on. In *Proceedings of the IEEE/CVF conference on computer vision and pattern recognition*, pages 2231–2235, 2022.

[27] Zixun Fang, Wei Zhai, Aimin Su, Hongliang Song, Kai Zhu, Mao Wang, Yu Chen, Zhiheng Liu, Yang Cao, and Zheng-Jun Zha. Vivid: Video virtual try-on using diffusion models. *arXiv preprint arXiv:2405.11794*, 2024.

[28] Na Zheng, Xuemeng Song, Zhaozheng Chen, Linmei Hu, Da Cao, and Liqiang Nie. Virtually trying on new clothing with arbitrary poses. In *Proceedings of the 27th ACM international conference on multimedia*, pages 266–274, 2019.

[29] Fei Shen, Xin Jiang, Xin He, Hu Ye, Cong Wang, Xiaoyu Du, Zechao Li, and Jinghui Tang. Imagdressing-v1: Customizable virtual dressing. In *AAAI Conference on Artificial Intelligence*, 2024. URL <https://api.semanticscholar.org/CorpusID:271244829>.

[30] Zijian He, Peixin Chen, Guangrun Wang, Guanbin Li, Philip HS Torr, and Liang Lin. Wildvidfit: Video virtual try-on in the wild via image-based controlled diffusion models. *arXiv preprint arXiv:2407.10625*, 2024.

[31] Ming Meng, Qi Dong, Jiajie Li, Zhe Zhu, Xingyu Wang, Zhaoxin Fan, Wei Zhao, and Wenjun Wu. Hf-vton: High-fidelity virtual try-on via consistent geometric and semantic alignment. *arXiv preprint arXiv:2505.19638*, 2025.

[32] Jascha Sohl-Dickstein, Eric Weiss, Niru Maheswaranathan, and Surya Ganguli. Deep unsupervised learning using nonequilibrium thermodynamics. In *International conference on machine learning*, pages 2256–2265. PMLR, 2015.

[33] Yang Song, Jascha Sohl-Dickstein, Diederik P Kingma, Abhishek Kumar, Stefano Ermon, and Ben Poole. Score-based generative modeling through stochastic differential equations. In *International Conference on Learning Representations*, 2021. URL <https://openreview.net/forum?id=PxtIG12RRHS>.

[34] Laurent Dinh, Jascha Sohl-Dickstein, and Samy Bengio. Density estimation using real nvp. *arXiv preprint arXiv:1605.08803*, 2016.

[35] Laurent Dinh, David Krueger, and Yoshua Bengio. Nice: Non-linear independent components estimation. *arXiv preprint arXiv:1410.8516*, 2014.

[36] Durk P Kingma and Prafulla Dhariwal. Glow: Generative flow with invertible 1x1 convolutions. *Advances in neural information processing systems*, 31, 2018.

[37] Tian Qi Chen, Yulia Rubanova, Jesse Bettencourt, and David Kristjanson Duvenaud. Neural ordinary differential equations. In *Neural Information Processing Systems*, 2018. URL <https://api.semanticscholar.org/CorpusID:49310446>.

[38] Yaron Lipman, Ricky T. Q. Chen, Heli Ben-Hamu, Maximilian Nickel, and Matt Le. Flow matching for generative modeling. *ArXiv*, abs/2210.02747, 2022. URL <https://api.semanticscholar.org/CorpusID:252734897>.

[39] Davide Morelli, Alberto Baldrati, Giuseppe Cartella, Marcella Cornia, Marco Bertini, and Rita Cucchiara. Ladi-nton: Latent diffusion textual-inversion enhanced virtual try-on. In *Proceedings of the 31st ACM international conference on multimedia*, pages 8580–8589, 2023.

[40] Gwanghyun Kim, Taesung Kwon, and Jong Chul Ye. Diffusionclip: Text-guided diffusion models for robust image manipulation. In *Proceedings of the IEEE/CVF conference on computer vision and pattern recognition*, pages 2426–2435, 2022.

[41] Junhong Gou, Siyu Sun, Jianfu Zhang, Jianlou Si, Chen Qian, and Liqing Zhang. Taming the power of diffusion models for high-quality virtual try-on with appearance flow. In *Proceedings of the 31st ACM International Conference on Multimedia*, pages 7599–7607, 2023.

[42] William Peebles and Saining Xie. Scalable diffusion models with transformers. In *Proceedings of the IEEE/CVF international conference on computer vision*, pages 4195–4205, 2023.

[43] Diederik P Kingma and Max Welling. Auto-encoding variational bayes. *arXiv preprint arXiv:1312.6114*, 2013.

[44] Alexey Dosovitskiy, Lucas Beyer, Alexander Kolesnikov, Dirk Weissenborn, Xiaohua Zhai, Thomas Unterthiner, Mostafa Dehghani, Matthias Minderer, Georg Heigold, Sylvain Gelly, et al. An image is worth 16x16 words: Transformers for image recognition at scale. *arXiv preprint arXiv:2010.11929*, 2020.

[45] Black Forest Labs. Flux. <https://github.com/black-forest-labs/flux>, 2024.

[46] Black Forest Labs, Stephen Batifol, Andreas Blattmann, Frederic Boesel, Saksham Consul, Cyril Diagne, Tim Dockhorn, Jack English, Zion English, Patrick Esser, Sumith Kulal, Kyle Lacey, Yam Levi, Cheng Li, Dominik Lorenz, Jonas Müller, Dustin Podell, Robin Rombach, Harry Saini, Axel Sauer, and Luke Smith. Flux.1 kontext: Flow matching for in-context image generation and editing in latent space, 2025. URL <https://arxiv.org/abs/2506.15742>.

[47] Xingchao Liu, Chengyue Gong, and Qiang Liu. Flow straight and fast: Learning to generate and transfer data with rectified flow. *arXiv preprint arXiv:2209.03003*, 2022.

[48] Edward J Hu, Yelong Shen, Phillip Wallis, Zeyuan Allen-Zhu, Yuanzhi Li, Shean Wang, Lu Wang, Weizhu Chen, et al. Lora: Low-rank adaptation of large language models. *ICLR*, 1(2):3, 2022.

[49] Shuai Bai, Keqin Chen, Xuejing Liu, Jialin Wang, Wenbin Ge, Sibo Song, Kai Dang, Peng Wang, Shijie Wang, Jun Tang, et al. Qwen2. 5-vl technical report. *arXiv preprint arXiv:2502.13923*, 2025.

[50] Jim Nilsson and Tomas Akenine-Möller. Understanding ssim. *arXiv preprint arXiv:2006.13846*, 2020.

[51] Richard Zhang, Phillip Isola, Alexei A Efros, Eli Shechtman, and Oliver Wang. The unreasonable effectiveness of deep features as a perceptual metric. In *Proceedings of the IEEE conference on computer vision and pattern recognition*, pages 586–595, 2018.

[52] Maximilian Seitzer. pytorch-fid: FID Score for PyTorch. <https://github.com/mseitzer/pytorch-fid>, August 2020. Version 0.3.0.

[53] Mikołaj Bińkowski, Danica J Sutherland, Michael Arbel, and Arthur Gretton. Demystifying mmd gans. *arXiv preprint arXiv:1801.01401*, 2018.

[54] Jianhao Zeng, Dan Song, Weizhi Nie, Hongshuo Tian, Tongtong Wang, and An-An Liu. Cat-dm: Controllable accelerated virtual try-on with diffusion model. In *Proceedings of the IEEE/CVF conference on computer vision and pattern recognition*, pages 8372–8382, 2024.

[55] Shitao Xiao, Yueze Wang, Junjie Zhou, Huaying Yuan, Xingrun Xing, Ruiran Yan, Chaofan Li, Shuteng Wang, Tiejun Huang, and Zheng Liu. Omnigen: Unified image generation. In *Proceedings of the Computer Vision and Pattern Recognition Conference*, pages 13294–13304, 2025.